SHAPE OF Fe-Ni GRAINS AND MAGNETIC SUSCEPTIBILITY ANISOTROPY IN ANTARCTIC CHONDRITES

Naoyuki FUJII, Keisuke ITO,

Department of Earth Sciences, Faculty of Science, Kobe University, 1-1, Rokkodai-cho, Nada-ku, Kobe 657

Masamichi MIYAMOTO

Department of Pure and Applied Sciences, College of General Education, University of Tokyo, 8-1, Komaba 3-chome, Meguro-ku, Tokyo 153

and

Yozo HAMANO

Geophysical Institute, Faculty of Science, University of Tokyo, 11-16, Yayoi 2-chome, Bunkyo-ku, Tokyo 113

Abstract: Magnetic susceptibility anisotropy is measured for various petrologic types of ordinary chondrites from Antarctica, which are three H types: ALH-77233 (H4), ALH-77182(H5) and ALH-77115(H6); four L types: Y-74191(L3), ALH-77230(L4), ALH-77254(L5) and ALH-77231(L6); and four LL types: Y-75258(LL6), Y-790519(LL), Y-790723(LL) and Y-790964(LL). The last three are shock-melted chondrites and have high strengths, whereas Y-75258 has a very low strength. Magnetic susceptibility anisotropy appears to be low for LL chondrites and seems to bear no correlation with porosity and petrologic types among H and L chondrites. Both prolate and oblate susceptibility ellipsoids are obtained. To characterize the shape irregularity of metallic grains, the Fourier descriptors representation with an arc-length coordinate system is introduced for two-dimensional outline of grains. Unlike the normally used polar coordinate system, this method is applicable to any complicated shape of grain boundary. Some advantages of the present method are demonstrated for several selected Fe-Ni grains from the same specimens as those used for the magnetic and the strength measurements. Newly proposed parameters representing deviations from circular and elliptical shapes are shown to distinguish different complex outlines of Fe-Ni grains.

1. Introduction

Chondrites are composed of more or less deformed or fragmented grains which may reflect the impact and lithification histories of chondrites (DODD, 1969, 1976; WASSON, 1972, 1974; BEVAN and AXON, 1980; SCOTT and RAJAN, 1981). The texture of metal grains in chondrites, such as the irregular shape (SCOTT, 1982; FUJII *et al.*, 1982, 1983) and anisotropic orientations (STACEY *et al.*, 1961; WEAVING, 1962; HAMANO and YOMOGIDA, 1982; SUGIURA and STRANGWAY, 1982) could provide some information about the degree of lithification or the strength as well as the evolutional process of

chondritic parent bodies (FUJII *et al.*, 1981c; HAMANO, 1982). For various petrologic types of H, L, and LL chondrites, we have studied the strength by means of the vibrational fracturing rate (VFR) method (FUJII *et al.*, 1980, 1981a; MIYAMOTO *et al.*, 1982) and the shape irregularity of Fe-Ni grains based on microscopic observations (FUJII *et al.*, 1982, 1983).

The magnetic susceptibility anisotropy represented as an ellipsoid would reflect the orientation distribution of Fe-Ni grains in each chondrite (HAMANO and YOMOGIDA, 1982). By using the same samples as those studied for the two-dimensional shape irregularity of Fe-Ni grains (FUJII *et al.*, 1982), the magnetic susceptibility ellipsoid is measured in this study. The ellipsoid approximation of the grain shape, however, should not be enough to characterize the specific material and to reflect the deformation of Fe-Ni grains involving such events as grain boundary diffusion and melting, impact and lithification processes. Because the actual shape of each Fe-Ni grain generally shows very complex outlines, quantitative description of the shape of such grains is required. The technique normally used in the grain shape analysis has been the Fourier series expansion of the radius as a function of polar angle (*e.g.* SCHWARCZ and SHANE, 1969). Because of the irregularity of the shape, this technique cannot be applied to Fe-Ni grains in chondrites. One of the Fourier descriptors (GRANLUND, 1972) is introduced to characterize the shape of Fe-Ni grains. In this study, some advantages of this procedure are demonstrated and new parameters of the shape irregularity are introduced to represent deviations from circular and elliptical outlines by applying them to several selected Fe-Ni grains.

2. Magnetic Susceptibility Anisotropy of Antarctic Chondrites

2.1. Samples and method of measurement

All samples of Antarctic chondrites are supplied by the National Institute of Polar Research. They include three H chondrites: ALH-77233 (H4), ALH-77182(H5) and ALH-77115(H6), four L chondrites: Y-74191(L3), ALH-77230(L4), ALH-77254 (L5), and ALH-77231(L6), and four LL chondrites: Y-75258(LL6), Y-790519(LL), Y-790723(LL), and Y-790964(LL), and their strengths have been previously measured by the VFR method (FUJII *et al.*, 1980, 1981a; MIYAMOTO *et al.*, 1982). The samples except three shock-melted LL chondrites in the Yamato-79 collection were embedded in a resin and a flat surface of at least 20 mm^2 is exposed in each sample which was of a rectangular shape with a volume of more than 0.5 cm^3. Because of the irregular shapes of samples, the actual volume of chondrites in the resin varies from 0.05 to 0.3 cm^3. Specimens used in this measurement are the same as the ones previously used in the microscopic grain shape analysis by FUJII *et al.* (1982), except for ALH-77231 (L6) and shock-melted LL chondrites.

Magnetic susceptibility anisotropy was measured by using a Shonstedt SSM-1A spinner magnetometer. Since five independent components of magnetic susceptibility tensor were obtained from a 6-spin measurement, full components were determined by measuring an absolute value for one of the three diagonal components by using a Bison susceptibility bridge. After correcting the effects of induced demagnetization, three principal components of intrinsic magnetic susceptibility and their orientations in the

coordinate system fixed to be parallel to each edge of the sample were calculated. The accuracy of magnetic susceptibility measurements depends on the volume and shape of samples and is about ± 5 percent for typical specimens studied. The description of this measurement has been given in more detail by HAMANO and YOMOGIDA (1982).

2.2. *Magnetic susceptibility anisotropy*

A measure of anisotropy in magnetic susceptibility is expressed as K1/K3, where K1 and K3 are the maximum and the minimum principal values of susceptibility, respectively. A type of anisotropy is expressed by using a parameter A, which is defined by $\tan^2 A=(K2-K3)/(K1-K2)$, where K2 is the intermediate principal value of susceptibility. When the susceptibility ellipsoid is prolate, the value of A varies from 0° to 45°, and when it is oblate, A varies from 45° to 90°. The values of K1/K3 and A (in degrees) are listed in Table 1. Volume fraction and the average shape parameters (SP) are also listed in Table 1, together with the logalithmic ratio of VFR to that of olivine (FUJII *et al.*, 1981a; MIYAMOTO *et al.*, 1982).

Table 1. Magnetic susceptibility anisotropy, volume fraction, and shape parameter (SP) of Fe-Ni grains, logalithmic ratio of VFR and porosity.

Sample	Fe-Ni grains				$\log(V/V_0)$[2]	Porosity
	K1/K3[3]	A[3]	(vol %)	SP[1]		
ALH-77233 (H4)	1.405	42.5	6.3	7.7	0.28	5
ALH-77182 (H5)	1.205	36.2	4.1	5.5	0.28	15
ALH-77115 (H6)	1.318	65.6	4.9	6.3	0.20	(8)
Y-74191 (L3)	1.792	47.0	7.1	6.4	0.24	—
ALH-77230 (L4)	1.475	44.7	8.8	6.5	0.13	1
ALH-77254 (L5)	1.642	42.9	4.0	6.8	−0.04	18
ALH-78105 (L6)	1.123	47.5	2.3	5.8	−1.07	4
ALH-77231 (L6)	1.574	34.4	1.4	6.4	−0.76	(3)
Y-75258 (LL6)	1.047	39.1	0.9	4.2	−1.08	(33)
Y-790519 (LL)	1.328	31.4	—	—	0.31	7
Y-790723 (LL)	1.096	49.4	—	—	0.30	8
Y-790964 (LL)	1.094	46.4	—	—	0.43	16

1) $SP=\langle\Sigma(L\cdot\sqrt{S})/\Sigma S\rangle$, where the summation is made over grains with the area S greater than 0.01 mm² (FUJII *et al.*, 1982).
2) V and V_0 are the values of VFR of sample and that of olivine single crystal, respectively (FUJII *et al.*, 1980, 1981a).
3) K1/K3 and A are parameters of magnetic susceptibility anisotropy and defined in text.
Note: the definition of SP shown above has changed from the previous work by FUJII *et al.* (1982).

Since the magnetic susceptibility ellipsoid would represent a volumetric average of the anisotropic shape of Fe-Ni grains, the orientation of this ellipsoid would be correlative with the orientation distribution of Fe-Ni grains from microscopic observations (FUJII *et al.*, 1982). By projecting the magnetic anisotropy ellipsoid to each sample surface, the orientation of the major axis a and the axial ratio $(a-b)/a$ are calculated, in which b is the minor axis. Star symbols in Fig. 1 indicate the orientation of a with $(a-b)/a$ as a radial distance of the magnetic susceptibility ellipse. A dashed line is

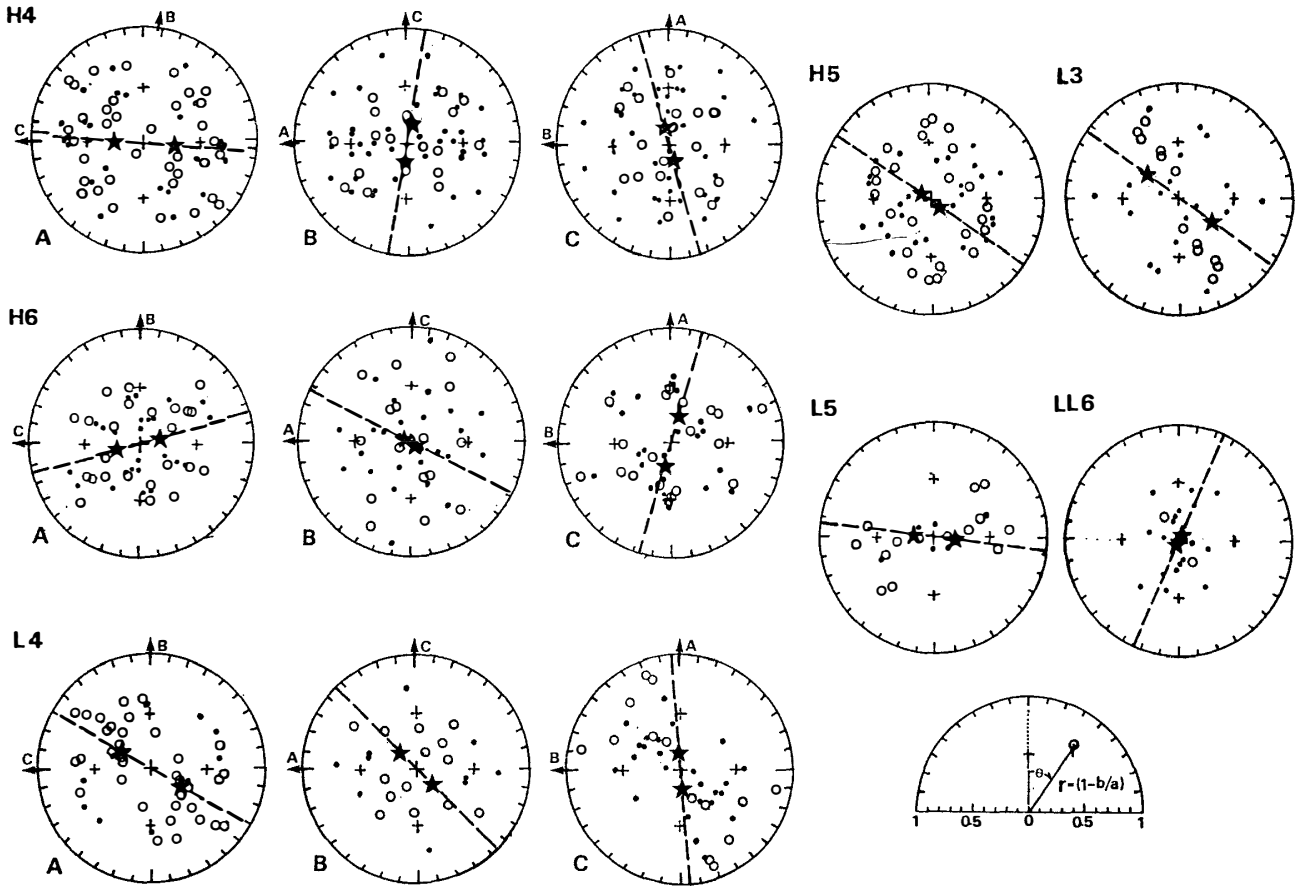

Fig. 1. A pair of star symbols and dashed line indicate the orientation of the major axis of the magnetic susceptibility ellipsoid projected to each sample surface. Open circles and dots are the orientations of the longest axis of Fe-Ni grains with the area larger and smaller than 0.01 mm², respectively, from FUJII et al. (1982). Chondrites shown are H4 (ALH-77233), H5 (ALH-77182), H6 (ALH-77115), L3 (Y-74191), L4 (ALH-77230), L5 (ALH-77254) and LL6 (Y-75258). The angle is measured clockwise from a coordinate system taken parallel to one of the edges of the specimen, and the radial distance is proportional to (a−b)/a, where a and b are major and minor axes of grain boundary curves, respectively. The diagrams labelled A, B and C for H4, H6 and L4 samples are the surfaces cut mutually perpendicular to each other as described in FUJII et al. (1982).

to indicate the orientation of the major axis more clearly. Open circles and dots in Fig. 1 represent the orientation distributions of the longest axis of Fe-Ni grains with an area larger and smaller than 0.01 mm^2, respectively, as previously obtained from microscopic observations by FUJII *et al.* (1982). The average orientation distribution of open circles and dots seems to be more or less correlated with that estimated from the magnetic susceptibility ellipsoid (stars), especially for the surfaces of L4-A and H6-A. Both estimations apparently coincide and show nearly isotropic orientations for the surfaces of H6-B, H5 and LL6. For the surfaces of L4-C, L3 and L5, however, the orientations of the major axis of susceptibility ellipsoid are oblique to those of the grain shape, in which the degree of anisotropy is relatively high.

3. Shape Analysis of Fe-Ni Grains

3.1. Fourier descriptors for plane closed curves

Among many techniques for describing plane closed curves, the Fourier descriptors are a useful set as evidenced both theoretically and experimentally (*e.g.* ZAHN and ROSKIES, 1972; GRANLUND, 1972; RICHARD and HEMAMI, 1974; PERSOON and FU, 1977). A plane closed curve, C, is characterized by a parametric representation $(X(l), Y(l))=Z(l)$, and $0\leq l\leq L$ where l is the clockwise arc length along C and L is the total perimeter length of C. The complex coordinate function $U(l)=X(l)+i\cdot Y(l)$ is periodic with period L and the Fourier descriptor can be represented by (GRANLUND, 1972; RICHARD and HEMAMI, 1974);

$$A_n=\frac{1}{L}\int_0^L U(l)\cdot\exp(-i\cdot 2\pi nl/L)\,\mathrm{d}l \qquad (1)$$

and

$$U(l)=\sum_{n=-\infty}^{\infty} A_n\cdot\exp(i\cdot 2\pi nl/L)\,. \qquad (2)$$

The piecewise smoothness of $U(l)$ is sufficient to insure that the Fourier series converges absolutely at any point l. A set of $\{A_n\}$ is called the Fourier descriptors which is independent of the choice of initial point, and invariant with respect to rotation and trans-

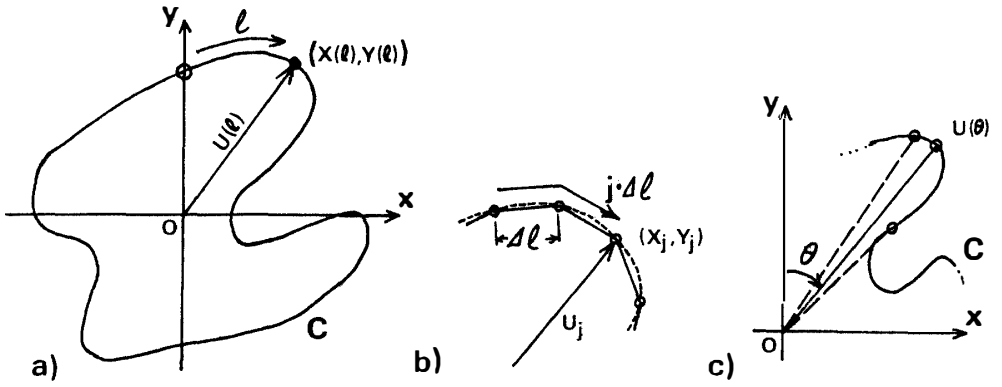

Fig. 2. a) An arc-length coordinate system for a closed boundary curve and the complex function $U(l)$. Open circle indicates the starting point. b) A polygon approximation with an equi-length line segment (Δl). c) A polar coordinate system for the complex function $U(\theta)$.

lation of the curve C as illustrated in Fig. 2a (ZAHN and ROSKIES, 1972; RICHARD and HEMAMI, 1974). The parameter l can be chosen to be proportional to arc length, *i.e.*, the velocity along C, dZ/dl, is a constant.

In practice, we approximate the plane closed curve with a polygon with N equi-length line segments (Δl) and the origin of the coordinate is taken to be the center of gravity. Then the complex function $U(l)$ is represented by a series of complex points U_j which can be expanded in a finite Fourier series;

$$\begin{aligned} U_j &= X_j + i \cdot Y_j , \qquad j = 1, 2, \ldots, N \\ &= \sum_{k=-M}^{M} A_k \cdot \exp(i \cdot 2\pi k \cdot j/N) , \end{aligned} \tag{3}$$

where $M=(N-1)/2$ and

$$A_k = \frac{1}{N} \sum_j U_j \cdot \exp(-i \cdot 2\pi k \cdot j/N) . \tag{4}$$

where k is the harmonic order and $l = j \cdot \Delta l$. The point (X_j, Y_j) is the terminal point of the $(j-1)$th line segment and the initial point of the jth line segment (Fig. 2b). For a demonstrative purpose, we tentatively use the amplitude spectrum B_k, which is the real part of A_k in eq.(4), and the radial distance function R_j which corresponds to U_j in eq.(3), *i.e.*;

$$R_j/R_0 = 1 + 2 \sum_{j=1}^{M} B_k \cdot \cos(k \cdot j/N - D_k) , \tag{5}$$

where R_0 and D_k are the average radius and phase angles, respectively. The amplitude spectrum of the radial distance function B_k could characterize the variety of the shape irregularity among Fe-Ni grains. The deviation of the actual outline from a circle of radius R_0 can be represented by $P = 2\sum_k B_k^2$. By analogy with the Fourier series expansion in a polar coordinate for nearly circular outlines, the second order of B_k ($k=2$) can be regarded as a component of ellipse. We introduce a new parameter Q defined by $P - 2 \cdot B_2^2$ which would approximately indicate the deviation of the curve from an ellipse. P and Q are independent of the size of grains and may be called non-circularity and non-ellipticity parameters, respectively. As the curve fits more closely to an ellipse, the the ellipse approaches zero. Then this parameter could indicate a degree of fitness to value of Q approximation used in the orientation distribution of major axis of grains.

To describe a two-dimensional outline of a grain, a finite Fourier series expansion is normally used in a polar coordinate system for the radial distance function $R(\theta)$, where θ is polar angle (*e.g.* SCHWARCZ and SHANE, 1969). One advantage in using the arc-length coordinate (along line segments of a polygon boundary) instead of the polar coordinate is that $U(l)$ is always a single-valued function with period L. There are many outlines where $U(\theta)$ in the polar coordinate becomes two-valued and cannot be expanded by the Fourier series (Fig. 2c). In such a case, one needs to introduce more complicated procedures, for example, a complicated plane closed curve is artifically subdivided into several curves, each of which can be expressed by a single-valued function. This procedure cannot be used in this study because the shape irregularity is greately modified and the characteristic feature of original grain boundaries is obviously lost. In addition, an equal division of the angle θ causes large errors in the polygon approximation of a nonpolygonal closed curve when the angle between θ and

the tangent of the boundary curve becomes small as illustrated in Fig. 2c.

Another Fourier descriptor often used is a tangent angle representation of the boundary curve (ZAHN and ROSKIES, 1972). The angle function is related to the derivative of the coordinate function, $Z(l)$, and is sensitive to the noise inherent in a fuzzy boundary (RICHARD and HEMAMI, 1974) especially for a polygon approximated boundary curve.

3.2. *Effects of polygon approximation on the Fourier descriptors*

For a reference example of the Fourier descriptors representation, an ellipse with $a/b=2$ is analyzed, where a (20 cm) and b (10 cm) are major and minor axes, respectively. The ratio of the perimeter length L to the square root of the area S (introduced by FUJII *et al.*, 1982) is 3.975. The boundary curve is manually digitized with resolution of 0.1 mm and an absolute accuracy of location is about 0.5 mm, by using a digitizer (Model DT-1000, Watanabe Sokki, Co.). The number of equi-length line seg-

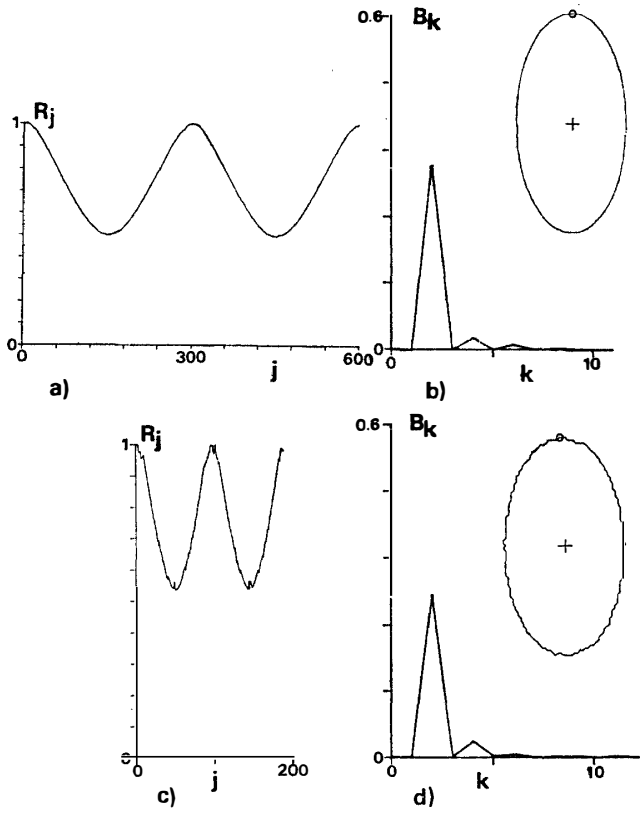

Fig. 3. a) The radial distance function R_j of an ellipse as a function of arc-length. Data are obtained by using a digitizer manually. b) The amplitude spectrum B_k of an ellipse. Actual shape of the digitized data is shown in the insert, where a plus symbol and a small circle indicate the origin of coordinate (the center of gravity) and the starting point ($j=0$), respectively. c) The radial distance function R_j of an ellipse by using a camera-image memory digitizing system with $N=200$. d) The amplitude spectrum, B_k, of an ellipse by the same digitizing procedure as in c). Others are the same as in b).

ments is taken to be about 600. The normalized radial distance function, R_j, from the center of gravity is shown as a function of boundary line length along the arc in Fig. 3a. The actual boundary line of the ellipse after digitized is illustrated in the insert in Fig. 3b, in which a plus symbol is the center of gravity. After subtracting the average radial distance from the R_j, the Fourier amplitude spectrum, B_k, of the ellipse is computed and illustrated in Fig. 3b, in which the vertical scale is normalized by the average radial distance. The largest peak represents the elongated feature of this ellipse. The second largest peak would come from the difference between the curvatures of peaks and valleys of R_j as seen in Fig. 3a. Other smaller peaks of higher wave number are considered to be due to a finite Fourier expansion and errors of the polygon approximation in the digitizing procedure.

To avoid probable errors or artificial noises in the manually digitizing process by using a desk-top digitizer, we examine another way of digitization by using a commercial TV camera with an image memory which is directly connected with a microcomputer. The boundary line thus digitized is illustrated in the insert in Fig. 3d. The same ellipse as that used in Fig. 3b is analyzed by this procedure, and the radial distance function and the Fourier amplitude spectrum are illustrated in Figs. 3c and 3d, respectively. Values of P and Q are 0.110 and 0.001 for Fig. 3b and 0.091 and 0.001 for Fig. 3d, respectively. Because of a limited size of memories (256×256 pixels in a frame), the number of segments is taken to be 200. Small notches and the differences of peaks and P values in Fig. 3c are due to noises and cut-off errors in the digitization. On the other hand, the amplitude spectrum in Fig. 3d and Q value are nearly the same as those in Fig. 3b. This may reflect the insensitivity of the Fourier descriptors to the noises inherent in such a fuzzy boundary. However, we cannot completely correct the distortion of the boundary curve due to the TV camera-image memory system for arbitrary magnification, and for more fuzzy boundary curves. A more reliable camera-memory system is needed for determination of actual boundaries of Fe-Ni grains.

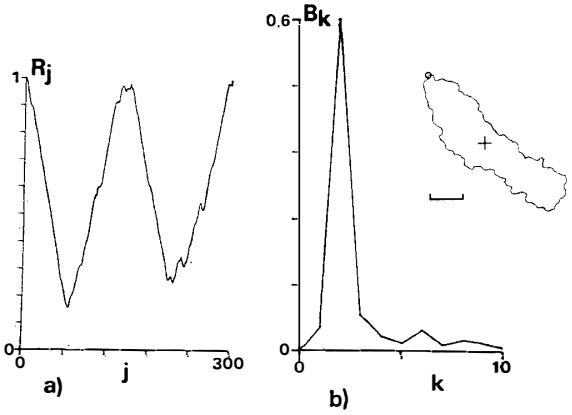

Fig. 4. a) The radial distance function R_j and b) the amplitude spectrum B_k for a Fe-Ni grain (A-13) from ALH-77230 (L4). A small bar in the insert corresponds to 1 cm in the photograph (×100). Other symbols are the same as in Fig. 3.

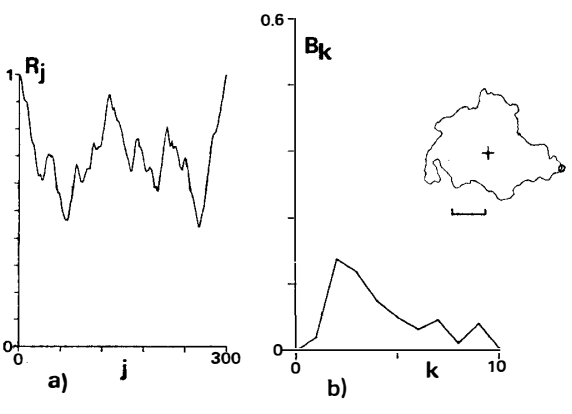

Fig. 5. a) The radial distance function R_j and b) the amplitude spectrum B_k for a Fe-Ni grain (C-23) from ALH-77233 (H4). Other symbols are the same as in Fig. 4.

3.3. *Examples of the Fourier descriptors for selected Fe-Ni grains*

To demonstrate the actual radial distance function R_j and its amplitude spectrum, B_k, five Fe-Ni grains are selected and manually digitized in the same manner as that described for Figs. 3a and 3b in the previous section. In Figs. 4 to 8, R_j and B_k are shown with an actual boundary curve in the insert.

Figures 4a and 4b demonstrate the radial distance function R_j and the amplitude spectrum, B_k of a Fe-Ni grain in ALH-77230(L4). Because the shape of this grain is similar to an ellipse as illustrated in the insert in Fig. 4b, R_j and B_k are essentially the same as those in Figs. 3a and 3b, respectively. One strong peak in Fig. 4b reflects the elongated shape of this grain and the distortion from an ellipse appeared in the different amplitude spectrum in the higher wave number, when compared with those in Fig. 3b. Figure 5 shows another example of a Fe-Ni grain selected from ALH-77233 (H4). Because of the relatively equi-dimensional shape, the amplitude spectrum has no strong peak when Fig. 5b is compared with Fig. 4b. For larger harmonic order ($k>7$), however, the peaks of B_k in Fig. 5b are slightly higher than those in Fig. 4b,

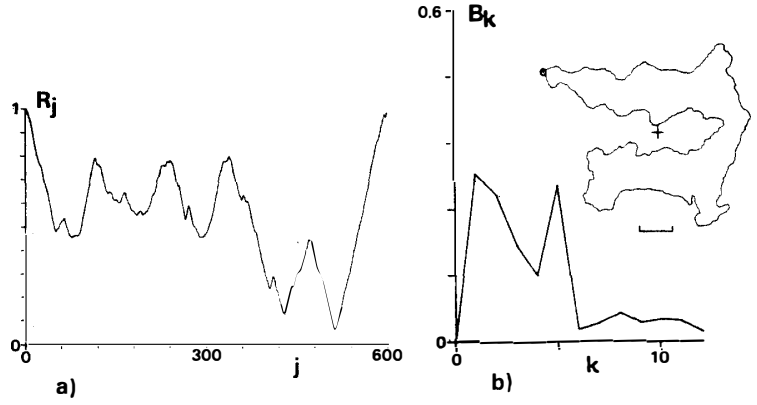

Fig. 6. a) The radial distance function R_j and b) the amplitude spectrum B_k for a Fe-Ni grain (A-11) from the surface A (Fig. 1) of ALH-77115 (H6). Other symbols are the same as in Fig. 4.

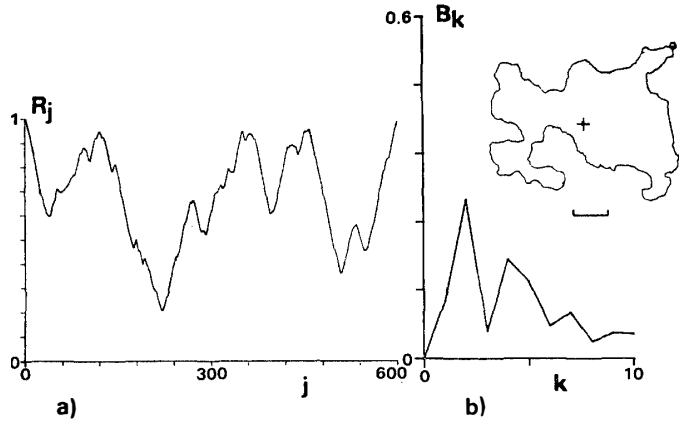

Fig. 7. A Fe-Ni grain (B-12) from the surface B (Fig. 1) of ALH-77115 (H6). Others are the same as in Fig. 6.

which would indicate the shape irregularity corresponding to these wave lengths is larger than that in Fig. 4. A horizontal bar is 0.1 mm in the actual specimen.

From ALH-77115(H6), three Fe-Ni grains are selected, each one from mutually perpendicular three surfaces, A, B and C which are included in Fig. 1, and the results of analysis are illustrated in Figs. 6, 7 and 8, respectively. A Fe-Ni grain from the surface A shown in Fig. 6 has a U-letter shape. Because the deviations from the average radial distance are biased in one direction from the origin of coordinate, the peak of $k=1$ in Fig. 6b becomes very strong. The second strongest peak ($k=5$) corresponds to the five peaks of R_j in Fig. 6a. For a Fe-Ni grain from the surface B (Fig. 7), the strongest peak in B_k is $k=2$, although the peak of $k=1$ is not weak either. The peak of $k=4$ is the second strongest in B_k (Fig. 7b). This may be due to the four peaks in R_j (Fig. 7a). Figure 8 shows an example of a Fe-Ni grain in the surface C in ALH-77115. Elongated feature of this grain reflects the strong peak in B_k ($k=2$) as seen in Fig. 8b. The difference between the actual grain shapes in Figs. 8b and 4b appears in the peak height in B_k for $k=5$ to 10.

As seen from Fig. 4 to Fig. 8, the variation of the shape of these Fe-Ni grains can be distinguished by the variety of different peaks in B_k. Although we cannot reproduce the original shape only from the amplitude spectrum, it is possible to distinguish various types of the shape irregularity in terms of relative height of peaks in B_k as a first step to characterize the shape of Fe-Ni grains. Values of parameters

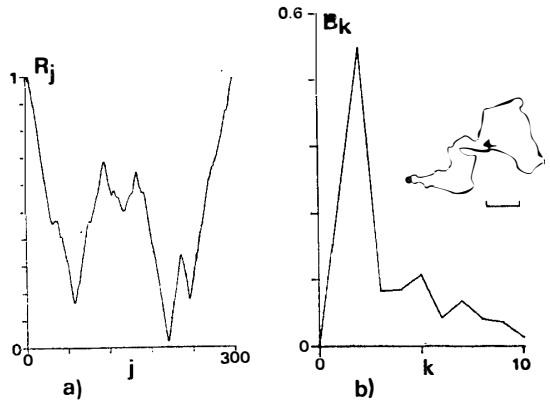

Fig. 8. A Fe-Ni grain (C-15) from the surface C (Fig. 1) of ALH-77115 (H6). Others are the same as in Fig. 6.

Table 2. Nondimensional parameters of the shape irregularity: $L/\sqrt{S}$, non-circularity (P), and non-ellipticity (Q) for selected Fe-Ni grains.

Sample	S (mm^2)	$L/\sqrt{S}$	P[1)]	Q[1)]
ALH-77230 (L4), A-13	6.0	5.8	0.37	0.01
ALH-77233 (H4), C-23	7.1	5.7	0.07	0.04
ALH-77115 (H6), A-11	13.6	9.1	0.30	0.25
ALH-77115 (H6), B-12	13.4	7.8	0.16	0.08
ALH-77115 (H6), C-15	3.9	7.2	0.41	0.12

1) $P=2\Sigma B_k^2$ and $Q=P-2\cdot B_2^2$, where B_k is the k-th order amplitude of the radius function defined in the text.

representing non-circularity, P, and non-ellipticity, Q, are listed in Table 2, together with values of S and $L/\sqrt{S}$. The characteristic feature of grain shape in the examples could be properly represented by these three parameters. For example, values of P and Q differ significantly between grains shown in Figs. 4 and 5, whereas values of $L/\sqrt{S}$ are similar to each other. In contrast, values of $L/\sqrt{S}$ are different among grains in Figs. 4, 6 and 8, while values of P are similar to each other, though values of Q differ to some extent.

It is noticed that all grains presented here cannot be analyzed by using a polar coordinate when the higher harmonic orders are intended to be included properly. For example, the radius function in a polar coordinate becomes two-valued and an equal division of the polar angle θ causes large differences in the lengths of segments of a polygon boundary, even for the nealy elliptic grain shown in Fig. 4.

4. Discussions and Conclusions

For all the samples studied, metal and sulfide grains generally exist at inter-chondrule spaces with irregular outlines except small inclusions of metallic phase in chondrules. The magnetic susceptibility ellipsoid would represent a measure of the volumetric average of orientation and shape distributions of Fe-Ni grains or other magnetic minerals in chondrites (*e.g.* STACEY *et al.*, 1961; HAMANO and YOMOGIDA, 1982). The magnetic susceptibility anisotropy K1/K3 obtained in this study ranges from 1.05 to 1.8 (Table 1) and seems to have little correlation with the porosity and petrologic types among H and L chondrites, unlike the porosity *vs.* K1/K3 relation among L chondrites postulated by HAMANO and YOMOGIDA (1982). However, the values of K1/K3 for LL chondrites are significantly smaller than that of others. This observation is concordant with a view that the shape of Fe-Ni grains becomes rounded as their size and content decrease (FUJII *et al.*, 1982). It is interesting to note that the shock-melted LL chondrites are in the highest strength group and LL6 (Y-75258) is in the lowest strength group (MIYAMOTO *et al.*, 1982) whereas both of them have low K1/K3 values. It may suggest that shock-induced melting would make metallic grains rounded. As noted by several authors (*e.g.* FUJII *et al.*, 1982; HAMANO and YOMOGIDA, 1982), the foliation (*i.e.* oblate ellipsoid; $45° \leq A \leq 90°$) is generally observed in chondrites including magnetic susceptibility anisotropy, petrofabric orientations of olivines and deformed chondrules. Types of magnetic susceptibility anisotropy obtained in this study, however, are both prolate and oblate (Table 1). It may be partly due to the inaccuracy of the susceptibility measurement for small volume (0.05 to 0.3 cm^3) and irregular shape of specimens. Values of the parameter A appear to have little correlation with porosity and petrologic type among chondrites studied.

The orientation distributions of the longest axis of Fe-Ni grains seem more or less to be correlated with the magnetic susceptibility ellipsoid measured for the same specimen for several surfaces of chondrites (Fig. 1). Some surfaces, however, show considerable discrepancies between the two estimates. As demonstrated in the previous section, the ellipse approximation sometimes deviates considerably due to the complicated shape of Fe-Ni grains. In addition, mutually perpendicular three surfaces of a specimen are cut in order to obtain the area of sample surface as large as pos-

sible so that the surfaces are oblique to the principal axes of magnetic susceptibility ellipsoid. All these factors are due to the small volume and irregular shape of specimens studied. There are, however, many difficulties to overcome for obtaining more quantitative correlations of magnetic susceptibility ellipsoids with the two-dimensional grain shape analysis, such as the fitness of ellipse approximation, homogeneity of grain distribution, and statistical approach to obtain bulk material properties. Further studies await more elabolate analyses to describe these irregular shapes and to provide a statistically meaningfull average of anisotropic orientation distributions of Fe-Ni grains.

The characteristic feature of Fe-Ni grains could be represented not only by the ellipsoid approximation but also by the shape irregularity (FUJII *et al.*, 1981b, 1982). Parameters of non-circularity P and non-ellipticity Q, together with $L/\sqrt{S}$ introduced in this study, are shown to be useful to characterize the grain shape other than the ellipsoid approximation, such as magnetic susceptibility anisotropy and orientation distribution of the major axis of grain boundaries. The technique normally used for the grain shape analysis has been the Fourier series expansion in polar coordinate system (*e.g.* SCHWARCZ and SHANE, 1969), which is applied, for example, to characterize the shape of meteoritic breccia and lunar soils (KORDESH, 1983). This technique, however, can only be applicable to nearly spherical (or nearly circular in two dimensions) grains, because the boundary surface (curve) function needs to be single-valued in this procedure, as pointed out in the previous section. The use of the Fourier descriptors, with arc-length coordinate system (*e.g.* PERSOONS and FU, 1977) introduced in this study makes it possible to apply the technique to any shape of grain boundary, as far as a simply connected closed curve in two dimensions is concerned. The amplitude spectrum and values of P and Q, together with the radial distance function, distinguish each Fe-Ni grain with respect to the harmonic order. Even when the lower order amplitude spectrum expresses a similar tendency, such as demonstrated for meteoritic breccias by KORDESH (1983), there remains a possibility that the discrimination between materials can be made by the higher harmonic order or by the relative differences among shape irregularity parameters introduced in this study.

Although the present investigation throws light on the quantitative analysis of complicated grain shape and the results for several selected grains are demonstrated, this procedure can easily be extended to a large number of Fe-Ni grains. Because mechanical histories of chondrites should be reflected in the texture and shape of composing grains to some extent, this method could also provide some clues to investigate the mechanisms of consolidation and lithification processes of chondrites and planetesimals (MIYAMOTO *et al.*, 1980; FUJII *et al.*, 1981b) and the fragmentation and brecciation processes of chondritic parent bodies (*e.g.* ITO *et al.*, 1982).

Acknowledgments

We thank the National Institute of Polar Research, Japan, for providing the chondrites from Antarctica. Thanks are also due to Drs. T. NAGATA, H. HASEGAWA, and H. TAKEDA who gave us helpful comments and suggestions. Critical comments by anonymous reviewers helped us to improve our manuscript. We appreciate Dr. K. DEGUCHI for his valuable suggestions about the shape analysis and Mr. Y. FURUKAWA

for his continuous assistance during the digitization and computation procedures. This work was supported in part by the Grant in Aid for Scientific Research from the Ministry of Education, Science and Culture, Japan. We are grateful to Ms. J. ASAKURA for typing the manuscript.

References

BEVAN, A. W. R. and AXON, H. J. (1980): Metallography and thermal history of the Tieschitz unequilibrated meteorite—Metallic chondrules and the origin of polycrystalline taenite. Earth Planet. Sci. Lett., **47**, 353–360.

DODD, R. T. (1969): Metamorphism of the ordinary chondrites; A review. Geochim. Cosmochim. Acta, **33**, 161–203.

DODD, R. T. (1976): Iron-silicate fractionation within ordinary chondrite groups. Earth Planet. Sci. Lett., **28**, 479–484.

FUJII, N., MIYAMOTO, M. and ITO, K. (1980): A new strength measure for ordinary chondrites. Mem. Natl Inst. Polar Res., Spec. Issue, **17**, 258–267.

FUJII, N., MIYAMOTO, M., KOBAYASHI, Y. and ITO, K. (1981a): Differences of relative strength among chondrites measured by the vibrational fracturing rate. Mem. Natl Inst. Polar Res., Spec. Issue, **20**, 362–371.

FUJII, N., MIYAMOTO, M., ITO, K. and KOBAYASHI, Y. (1981b): Effects of minor components on the consolidation of planetesimals and chondrites. Mem. Natl Inst. Polar Res., Spec. Issue, **20**, 372–383.

FUJII, N., HAMANO, Y. and MIYAMOTO, M. (1981c): Thermal stress in ordinary chondrite parent body; A possible cause of its lithification. Proc. 14th ISAS Lunar Planet. Symp. Tokyo, Inst. Space Astronaut Sci., 211–218.

FUJII, N., MIYAMOTO, M., KOBAYASHI, Y. and ITO, K. (1982): On the shape of Fe-Ni graines among ordinary chondrites. Mem. Natl Inst. Polar Res., Spec. Issue, **25**, 319–330.

FUJII, N., MIYAMOTO, M., KOBAYASHI, Y. and ITO, K. (1983): Anisotropic shape of Fe-Ni grains in ordinary chondrites. Lunar and Planetary Science XIV. Houston, Lunar Planet. Inst., 223–224.

GRANLUND, G. H. (1972): Fourier preprocessing for hand print character recognition. IEEE Trans. Comput., **21**, 195–201.

HAMANO, Y. (1982): Formation of ordinary chondrites: Evidence from the study of magnetic anisotropy and porosity. Formation of Planetesimals and Protoplanets, ed. by M. OJIMA. 100–108 (Progress Rep. of WG-4).

HAMANO, Y. and YOMOGIDA, K. (1982): Magnetic anisotropy and porosity of Antarctic chondrites. Mem. Natl Inst. Polar Res., Spec. Issue, **25**, 281–290.

ITO, K., FUJII, N., MIYAMOTO, M. and KOBAYASHI, Y. (1982): Mass and shape distributions of the Antarctic meteorites and low-velocity impact experiments. Proc. 15th ISAS Lunar Planet. Symp. Tokyo, Inst. Space Astronaut. Sci., 164–173.

KORDESH, K. (1983): Comparative Fourier grain shape analysis of meteoritic breccias and lunar soils. Lunar and Planetary Science XIV. Houston, Lunar Planet. Inst., 387–388.

MIYAMOTO, M., ITO, K., FUJII, N. and KOBAYASHI, Y. (1980): The significance of low melting-temperature materials in consolidation of planetesimals. Proc. 13th Lunar Planet. Symp. Tokyo, Inst. Space Aeronaut. Sci., Univ. Tokyo, 232–238.

MIYAMOTO, M., FUJII, N., ITO, K. and KOBAYASHI, Y. (1982): The fracture strength of meteorites; Its implication for their fragmentation. Mem. Natl Inst. Polar Res., Spec. Issue, **25**, 331–343.

PERSOON, E. and FU, K-S. (1977): Shape discrimination using Fourier descriptors. IEEE Trans. Syst., Man Cybern., **7**, 170–179.

RICHARD, C. W. and HEMAMI, H. (1974): Identification of three-dimensional objects using Fourier descriptors of the boundary curve. IEEE Trans. Syst., Man Cybern., **4**, 371–378.

SCHWARCZ, H. P. and SHANE, K. C. (1969): Measurement of particle shape by Fourier analysis. Sedimentology, **13**, 213–231.

SCOTT, E. R. D. (1982): Origin of rapidly solidified metal-troilite grains in chondrites and iron meteorites. Geochim. Cosmochim. Acta, **46**, 813–823.

SCOTT, E. R. D. and RAJAN, R. S. (1981): Metallic minerals, thermal histories and parent bodies of some xenolithic, ordinary chondrite meteorites. Geochim. Cosmochim. Acta, **45**, 53–67.

STACEY, F. D., LOVERING, J. F. and PARRY, L. G. (1961): Thermomagnetic properties, natural magnetic moments, and magnetic anisotropies of some chondritic meteorites. J. Geophys. Res., **66**, 1523–1534.

SUGIURA, N. and STRANGWAY, D. W. (1982): Magnetic properties of primitive non-carbonaceous chondrites. Mem. Natl Inst. Polar Res., Spec. Issue, **25**, 260–280.

WASSON, J. T. (1972): Formation of ordinary chondrites. Rev. Geophys. Space Phys., **10**, 711–749.

WASSON, J. T. (1974): Meteorites. New York, Springer, 316 p.

WEAVING, B. (1962): Magnetic anisotropy in chondritic meteorites. Geochim. Cosmochim. Acta, **26**, 451–455.

ZAHN, C. T. and ROSKIES, R. Z. (1972): Fourier descriptors for plane closed curve. IEEE Trans. Comput., **21**, 269–281.

(*Received June 20, 1983; Revised manuscript received October 19, 1983*)